JACS
JOURNAL OF THE AMERICAN CHEMICAL SOCIETY

Article

pubs.acs.org/JACS

Control of the Redox Activity of Quantum Dots through Introduction of Fluoroalkanethiolates into Their Ligand Shells

David J. Weinberg, Chen He, and Emily A. Weiss*

Department of Chemistry, Northwestern University, 2145 Sheridan Road, Evanston, Illinois 60208, United States

Supporting Information

ABSTRACT: Increasing the fraction of 1*H*,1*H*,2*H*,2*H*-perfluorodecanethiol (PFDT) in the mixed-PFDT/oleate ligand shell of a PbS quantum dot (QD) dramatically reduces the permeability of the ligand shell to alkyl-substituted benzoquinones (s-BQs), as measured by a decrease in the efficiency of collisional photoinduced electron transfer. Replacing only 21% of the oleates on the QD surface with PFDT reduces the yield of photo-oxidation by tetramethyl BQ by 68%. Experiments with s-BQ quenchers of two different sizes reveal that the degree of protection provided by the PFDT-doped monolayer, relative to a decanethiolate (DT)-doped monolayer at similar coverage, is due to both size exclusion (PFDT is larger and more rigid than DT), and the oleophobicity of PFDT. This work demonstrates the usefulness of fluorinated ligands in designing molecule-selective and potentially corrosion-inhibiting surface coatings for QDs for applications as robust emitters or high fidelity sensing platforms.

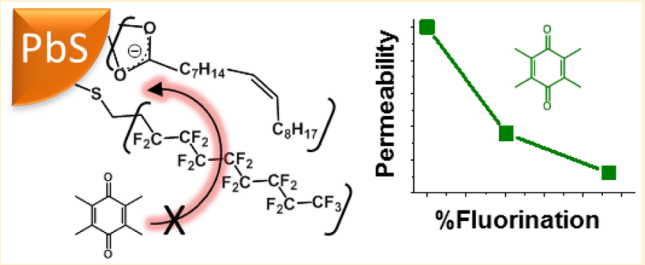

INTRODUCTION

Modification of the organic adlayer on the surface of a semiconductor nanocrystal (or quantum dot, QD) is a convenient and versatile method for controlling the interactions at the interface of the QD core and its surrounding environment.[1−5] If QDs are to be used in analytical or therapeutic applications, surface chemistries must be developed that not only promote targeted binding, but also minimize nonspecific interactions that contribute to "false positives", reduce the signal-to-noise ratio of the sensor,[1,2,6−10] and corrode the particle. The specificity of a QD's interaction with its environment is enhanced if the permeability of the ligand coating is sensitive to both the size and the chemical structure of small-molecule analytes or potential adsorbates. Here, we show that incorporating a partially fluorinated ligand, 1*H*,1*H*,2*H*,2*H*-perfluorodecanethiol (PFDT) into a small fraction of the organic adlayer of a near-infrared-emitting PbS QD dramatically reduces the efficiency of photo-oxidation of the QD by both 2,3,5,6-tetramethyl-*p*-benzoquinone (Me_4BQ) and 2,6-dimethyl-*p*-benzoquinone (Me_2BQ), due to a decrease in the permeability of the ligand shell to those small molecules.

A starting point for understanding the properties of the ligand shell that passivates and solubilizes a colloidal QD is to understand the properties of self-assembled monolayers (SAMs) on planar surfaces.[3,11,12] For planar surfaces, it has been shown that the intermolecular structure and order of a SAM comprising a mixture of organic molecules are sensitive to the mixed monolayer composition,[13−15] which can be used to tune its permeability to charged species[16] or to inhibit nonspecific protein binding.[10,17,18] The protective properties of the SAM are related to the chemical structure of its components;[12,19−22] for example, SAMs consisting of fluorinated molecules (FSAMs) are less permeable to small molecules than their aliphatic counterparts, and also exhibit weaker surface interactions with both polar and nonpolar liquids.[20,23−32] The blocking nature of fluorinated materials, which has been used to achieve resistance to corrosion, superior antifouling properties, or enhanced lubrication/liquid repellence,[33−37] is usually ascribed to (i) weak dispersive interactions caused by the low polarizability of the fluorine atom[23,38,39] and, particularly in the case of FSAMs, (ii) an improvement in the packing order and density due to the bulkiness of fluorocarbon molecules relative to their hydrocarbon analogues.[20,23−29,31,32] The extent to which each of these phenomena controls the behavior of FSAMs is an ongoing discussion in the literature.[24,39,40]

Recently, QDs coupled with fluorinated surfactants and polymers have been used as oxidation-resistant, IR-absorbing coatings[41] and robust emitters,[42,43] and are being investigated as multimodal optical/^{19}F MRI imaging platforms.[44−46] To develop further these emerging applications of fluorinated QDs, one cannot rely solely on the extensive fundamental research on the properties of FSAMs on planar metal surfaces,[23,24,26−29,39,47] because the nanoscale environments that control molecular ordering are fundamentally different on planar and nanoparticle surfaces. Specifically, we[48] and others[49] have demonstrated that alkyl ligands on a nanocrystal surface are more disordered than those on a flat metal substrate due to both the radius of curvature of the nanocrystal and the chemical heterogeneity of the nanocrystal surface. Although the synthesis

Received: December 14, 2015
Published: January 28, 2016

DOI: 10.1021/jacs.5b13077
J. Am. Chem. Soc. 2016, 138, 2319−2326

Table 1. Compositions of the Mixed Monolayers of OA/DT and OA/PFDT on PbS QDs after Thiol Treatment

equiv DT or PFDT added to OA-coated PbS QDs	bound OA/QD[a,e]	displaced OA/QD[a,e]	bound PFDT/QD[b,e]	bound DT/QD[c,e]	no. thiolate (DT or PFDT)/nm^2[d,e]	no. total ligands (OA + thiolate)/ nm^2[d,e]
0 DT/0 PFDT	220 ± 20	0	0	0	0	6.7 ± 0.7
24 DT	160 ± 10	47 ± 5	0	18 ± 1	0.50 ± 0.04	5.5 ± 0.4
48 DT	130 ± 10	90 ± 10	0	41 ± 1	1.14 ± 0.04	5.5 ± 0.4
30 PFDT	170 ± 10	52 ± 6	22 ± 1	0	0.62 ± 0.04	5.8 ± 0.4
60 PFDT	130 ± 10	90 ± 10	52 ± 4	0	1.4 ± 0.1	5.7 ± 0.5

[a]Calculated by integrating the bound and free oleate ^{1}H NMR signal from spectra of QDs treated with thiol, as described in the Supporting Information. [b]Calculated by integrating the PFDT CF_3 ^{19}F NMR signal as described in the text. [c]Estimated as the number of added DT per QD minus twice the number of DT disulfides formed. [d]Defined as the number of bound thiolates (or total bound ligands) per unit surface area, where surface area is 32.2 nm^2 as estimated from nanocrystal radius. [e]All errors estimated from NMR calibration curves as described in the Supporting Information, Figure S5.

of silicon nanoparticles with fluorinated monolayers and the effectiveness of these monolayers for inhibiting oxidative corrosion has been demonstrated,[43] mechanistic studies of monolayers containing fluorinated ligands on nanoparticle surfaces have so far been limited to a few investigations of solution-phase metal nanocrystals, which differ from semiconductor QDs in surface chemistry and surface structure.[43,50−54]

In this work, we quantitatively analyze the permeability of partially fluorinated SAMs on the surfaces of PbS QDs by monitoring the efficiency of collisionally gated photoinduced electron transfer from the QD to an alkyl-substituted benzoquinone (s-BQ). The s-BQ molecule must diffuse through the ligand shell within the lifetime of the PbS exciton in order to extract an electron from the QD core, so the yield of electron transfer is a direct measure of the ligand shell's permeability.[3,11,55] We find that PFDT dramatically reduces this permeability, even when it occupies a small fraction of the ligand shell, due to both its large molecular volume and conformational rigidity[23,24,26,27,29] and its oleophobicity. This result is an exciting step toward the use of QD ligand shells for chemical and size-based recognition of solution-phase analytes (an application of fluorinated QDs that has not yet been explored), and for protection of the QD core from redox-mediated corrosion.

RESULTS AND DISCUSSION

Compositions of the Mixed-Monolayer Ligand Shells of PbS QDs. We used a literature procedure adapted from Hines and Scholes[56] to synthesize PbS QDs with a first excitonic absorption at 985 nm, a radius of 1.6 nm (as determined from the sizing curve of Moreels et al., Figure S1 in the Supporting Information),[57] and coated with oleate (OA) ligands. We prepared samples of QDs that are coated with mixed monolayers of decanethiolate and oleate (DT/OA) or with mixed monolayers of perfluorodecanethiolate and oleate (PFDT/OA) by adding either DT or PFDT to dispersions of the oleate-coated QDs in deuterated benzene (for NMR characterization) or benzene (for optical characterization), and allowing the mixtures to sit for 12 h under ambient conditions. All thiol-treated QDs were prepared and stored under inert atmosphere in order to minimize the oxygen-catalyzed formation of disulfide species.

Table 1 summarizes the compositions of the ligand shells for the DT/OA-coated QD samples. The decanethiolate signal (2.18 ppm) corresponding to freely diffusing DT shown in Figure 1A disappears upon the addition of 24 or 48 equiv of DT to PbS QDs, which is expected for the signals of protons close to

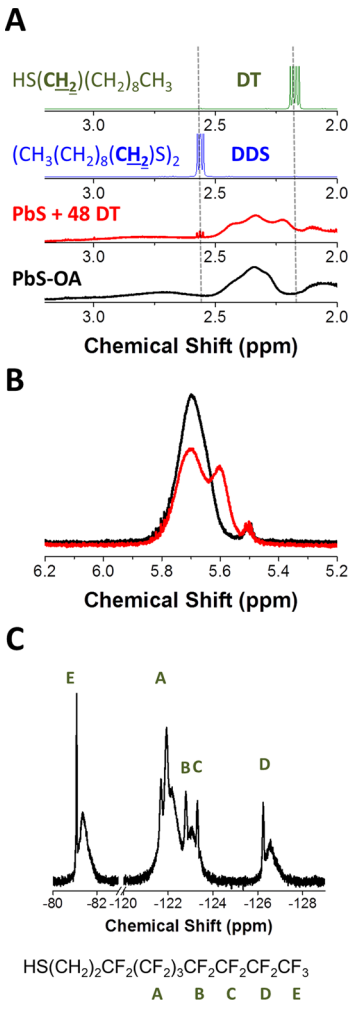

Figure 1. (A) ^{1}H NMR spectra of decanethiol (DT), decyl disulfide (DDS), oleate-coated PbS QDs treated with 48 mol equiv of DT, and oleate-coated PbS QDs in benzene-d_6. Bolded protons correspond to the signals shown in the spectra for DT and DDS. (B) Vinyl proton region of the ^{1}H NMR spectra the QD samples described in (A), with the same color code. The decrease in the signal from bound oleate at 5.68 ppm and the increase in signal from displaced oleate at 5.59 ppm upon addition of 48 equiv of DT shows that DT displaces oleate on the QD surface. The peak corresponding to displaced oleate is broadened due to fast exchange between free and bound states. The sharp signal at 5.5 ppm in both spectra corresponds to oleic acid molecules that are not in exchange with the PbS QD surface. (C) ^{19}F NMR spectra of the same PbS QDs treated with 60 mol equiv PFDT in benzene-d_6. Broad signals correspond to fluorines in bound PFDT, while sharp signals are free PFDT ligand, as labeled.

DOI: 10.1021/jacs.5b13077
J. Am. Chem. Soc. 2016, 138, 2319−2326

the surface of slowly diffusing nanocrystals.[58,59] There is, however, a clearly resolved signal corresponding to decyl disulfide that appears following the addition of 24 or 48 equiv of DT to PbS QDs, Figure 1A. This signal is not present in solutions of DT in the absence of PbS QDs, which indicates that a small fraction of the bound decanethiolate is oxidized to its disulfide and desorbs from the surface. We estimate the number of bound thiolates per QD using the fact that all added DT molecules either bind to the QD surface or are converted into free disulfides, and then subtracting the concentration of disulfide (measured from the integrated intensity of its NMR signal relative to a biphenyl standard) from the concentration of added DT, Table 1 (Figure S2 in the Supporting Information). We measured the concentration of displaced native ligand (OA) for each number of bound DT by integrating the vinyl ^{1}H NMR signals from bound and free OA in a process described in detail in the Supporting Information (Figure 1B, and the Supporting Information, Figure S3).[59,60] Each bound DT displaces, on average, at least two oleate ligands, presumably in the form of $Pb(OA)_2$ or Pb_xOA_y complexes, which are soluble in benzene. We note that the lead atoms displaced from the surface in the form of these complexes are likely not part of the inorganic core of the PbS nanocrystal, but are instead labile "Z-type" (neutral lead oleate) ligands that are in fast exchange with the QD surface. We do not observe any etching of the QDs in the form of a shift of their optical spectra to higher energy upon addition of thiols (see the Supporting Information, Figure S6).[61,62]

Table 1 also lists the composition of the PFDT/OA mixed monolayers on the PbS QDs. Unlike DT, we can directly quantify the number of bound PFDT per QD by ^{19}F NMR using the signal of the terminal CF_3 group of PFDT at −81.3 ppm (Figure 1C). We integrate the broad and sharp signals (corresponding to bound plus free PFDT) centered at −81.3 ppm, and compare this integral to that of the broad signal alone (see the Supporting Information, Figure S4) to obtain the fraction of PFDT that is bound. We then multiply this fraction by the number of equivalents of PFDT added to determine the number of bound PFDT ligands per QD, Table 1. As in the DT case, we also count displaced OA ligands relative to an internal biphenyl standard via ^{1}H NMR, and we observe that each PFDT molecule displaces ∼2 oleates upon binding, probably again in the form of $Pb(OA)_2$ or Pb_xOA_y.

Influence of Fluorination on the Permeability of the Ligand Shell to Substituted Benzoquinones. We prepared a series of PbS QDs in benzene coated with DT/OA and PFDT/OA mixed monolayers in which there are 0.50 DT/nm^2, 1.14 DT/nm^2, 0.62 PFDT/nm^2, or 1.40 PFDT/nm^2 on the QD surface, Table 1. We note that the total ligand densities of all thiol-treated QDs (i.e., thiolate + OA) are the same within the error of the NMR measurements, Table 1. We used substituted benzoquinones (s-BQ) as a molecular probe of the relative permeabilities of these mixed monolayers because we[11,55,63] and others[64−67] have shown previously that an s-BQ quenches the PL of a QD through photoinduced electron transfer if it is able to diffuse through the QD's ligand shell and adsorb, either statically or transiently, to the QD surface. This electron transfer has a driving force of 0.05 eV for Me_4BQ and 0.25 eV for Me_2BQ, while both energy and hole transfer are highly energetically unfavorable.[11,55] We added varying amounts of either Me_4BQ or Me_2BQ to a stock solution of the thiol-treated QDs such that we created a set of samples with the same concentration of QDs but different concentrations of substituted benzoquinone (s-BQ).

Figure 2A shows the photoluminescence (PL) spectra of PbS QDs coated exclusively with OA following the addition of 0−2190 mol equiv of Me_4BQ. The Supporting Information contains these spectra for all monolayer compositions with both the Me_4BQ and Me_2BQ quencher (see the Supporting Information, Figures S7 and S8). The integrated PL intensity of the QDs always decreases with increasing concentrations of added s-BQ. We monitored the dynamics of the excited state of the QD using nanosecond-to-microsecond time scale transient absorption experiments on the same set of samples. Figure 2 shows that the decay of the excited state of the oleate-capped QDs monitored using the recovery of the ground state bleach (GSB) at 990 nm, accelerates with increasing concentration of added s-BQ (Figure 2C). We observe the same trend for all PFDT/OA-coated QDs and both s-BQ quenchers, see the Supporting Information (Figure S9). Each of these kinetic traces fits well to a monoexponential decay convoluted with a Gaussian instrument response function, with time constants listed in the

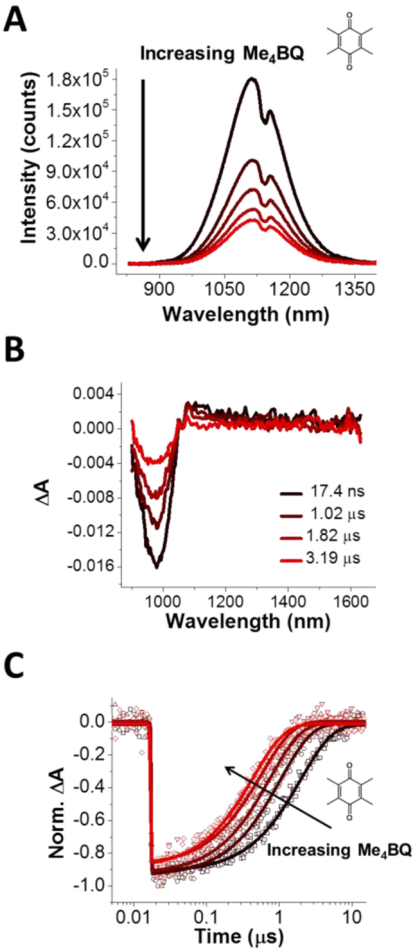

Figure 2. (A) Photoluminescence spectra of PbS QDs (11.5 μM) coated with oleate, after the addition of 0−2190 mol equiv of Me_4BQ, following photoexcitation at 800 nm. The "dip" at 1120 nm is attenuation due to absorption of a vibrational overtone of the solvent, benzene. (B) Transient absorption spectra of OA-coated PbS QDs (11.5 μM in benzene) at various delay times following photoexcitation at 850 nm. (C) Kinetic traces extracted at 990 nm (the peak of the ground state bleach) from the TA spectra of the PbS QD samples after the addition of 0−2190 mol equiv of Me_4BQ following photoexcitation at 850 nm. Solid lines are fits of the data to monoexponential decay convoluted with a Gaussian IRF.

DOI: 10.1021/jacs.5b13077
J. Am. Chem. Soc. 2016, 138, 2319−2326

Supporting Information (Table S3). The linear relationship between the concentration of added s-BQ and the rate of excited state decay (see the Supporting Information, Table S6) further indicates that the PL quenching is not due to disruption of the QD surface chemistry or the introduction of trap states, but is instead due to charge transfer.[11,55]

We then define the parameter "PL_0/PL", which is the ratio of the integrated PL intensity of each QD sample with no added s-BQ to the integrated PL intensity of the sample at each concentration of added s-BQ quencher. Figure 3A,B contains plots of PL_0/PL for QDs with the mixed monolayers PFDT/OA for Me_4BQ and Me_2BQ. The analogous plots for QDs coated by mixed monolayers of DT/OA are in Figure 3C,D. All plots of PL_0/PL are well fit ($r^2 > 0.98$) by the Stern–Volmer equation (eq 1), in which k_q is the bimolecular quenching rate constant and

$$\frac{PL_0}{PL} = 1 + k_q\tau_0[BQ] \quad (1)$$

τ_0 is the lifetime of the lowest-energy excitonic state of the QD in the absence of quencher, which we measured by TA. Table 2 lists the values of τ_0 for each QD sample, and the values of k_q for each type of mixed monolayer and each quencher.

The linear relationship between [s-BQ] and PL_0/PL (Figure 3) indicates that the quenching of the PbS excitonic state is dominated by diffusion-controlled electron transfer—that is, electron transfer between the QD and freely diffusing Me_4BQ or Me_2BQ molecules.[11,55] Interfacial charge transfer within static QD-molecule complexes typically occurs on the picosecond time scale.[11,55,68] We observe no picosecond-time scale dynamics of the QD's ground state bleach upon addition of the s-BQs to PFDT/OA-coated QDs or upon addition of Me_4BQ to oleate-coated QDs (Figures S11 and S12), and only a small (~10%) population of oleate-capped QDs undergo static quenching by Me_2BQ molecules preadsorbed to the nanocrystal surface (see Figures S11A and S12A), as we have seen previously.[11] We did not perform TA measurements on the mixtures of DT/OA-coated QDs with the s-BQs, but given that (i) incorporating DT into the PbS QD ligand shell consistently reduces the extent of PL quenching, in general, by s-BQs as shown in Figure 3, and (ii) we have shown previously that replacing oleate with DT on the surface of PbS QDs shuts off static quenching by an aminoferrocene redox partner,[69] we assume that any static quenching that exists in the case of oleate-capped QDs, which is almost negligible itself, would only be reduced upon the addition of decanethiolate to the QD ligand shell. For all mixed monolayers samples, then, in order to quench the PL of the QDs through the collisionally gated process, a diffusing BQ molecule must permeate the ligand shell during the lifetime of the exciton and position itself within a few angstroms of the QD core.[3,11,55,68] The extent to which Me_4BQ or Me_2BQ quenches the emission of PbS QDs is therefore a metric for the permeability of the monolayers to the s-BQ molecules.

To compare the permeabilities of mixed monolayer systems with different compositions, we calculate the collisional quenching efficiency, Φ_{coll}, of each QD-BQ system. Φ_{coll} is the fraction of collisions between the QD and s-BQ that result in

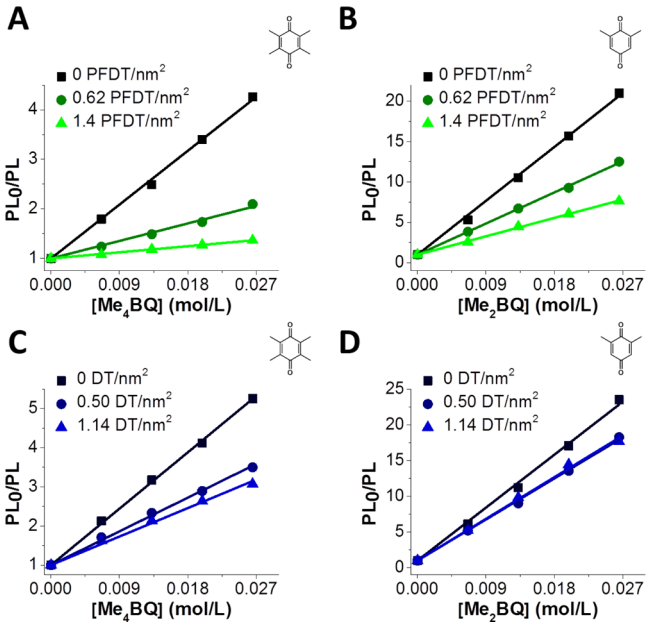

Figure 3. (A) Plot of PL_0/PL (solid symbols) for PbS QDs (11.5 μM in benzene) in which the PbS QDs are coated with OA (black), 0.62 PFDT/nm^2 (dark green), or 1.4 PFDT/nm^2 (light green) versus the concentration of Me_4BQ quencher. Solutions were photoexcited at 800 nm, and PL curves were collected 12 h after addition of 0–2190 equiv of Me_4BQ per QD. Colored lines correspond to fits to eq 1. **B)** Plot of PL_0/PL (solid symbols) for PbS QDs (11.5 μM in benzene) for the samples described in (A) versus the concentration of Me_2BQ quencher. Solutions were photoexcited at 800 nm, and PL curves were collected 12 h after addition of 0–2190 equiv of Me_2BQ per QD. Colored lines correspond to fits to eq 1. (C) Plot of PL_0/PL for PbS QDs (11.5 μM in benzene) in which the PbS QDs are coated with OA (black) 0.50 DT/nm^2 (dark blue), 1.14 DT/nm^2 (light blue) versus the concentration of Me_4BQ quencher. Colored lines correspond to fits to eq 1. (D) Plot of PL_0/PL for the samples described in (C) versus the concentration of Me_2BQ quencher. Colored lines correspond to fits to eq 1.

Table 2. Me_4BQ and Me_2BQ Quenching Parameters for PbS Coated with Thiolate-OA Ligand Shells

			Me_4BQ		Me_2BQ	
no. thiolate/nm^2	τ_0 (μs)[a]	k_0 (M^{-1} s^{-1})[b] ($\times 10^{10}$)	k_q (M^{-1} s^{-1})[c] ($\times 10^7$)	Φ_{coll} ($\times 10^{-4}$)	k_q (M^{-1} s^{-1})[c] ($\times 10^8$)	Φ_{coll} ($\times 10^{-4}$)
0 PFDT/DT	1.92 ± 0.02	9.5 ± 0.3	6.3 ± 0.1	7 ± 1[d]	3.9 ± 0.1	40 ± 4[d]
0.62 PFDT	1.80 ± 0.03	9.2 ± 0.3	2.2 ± 0.1	2.4 ± 0.1[e]	2.4 ± 0.1	26 ± 1[e]
1.4 PFDT	1.80 ± 0.02	9.6 ± 0.5	0.77 ± 0.01	0.80 ± 0.04[e]	1.41 ± 0.02	14.8 ± 0.8[e]
0.50 DT	1.69 ± 0.04	9.6 ± 0.4	5.6 ± 0.1	5.9 ± 0.3[e]	3.8 ± 0.1	40 ± 2[e]
1.14 DT	1.69 ± 0.03	9.2 ± 0.3	4.7 ± 0.1	5.1 ± 0.2[e]	3.8 ± 0.1	42 ± 2[e]

[a]Error of monoexponential fits of the recovery of the PbS QD ground state bleach, see the Supporting Information. [b]Error propagated from fitting DOSY data, see the Supporting Information, Figure S13. [c]Error propagated from error in τ_0 and in the linear fits presented in Figure 3. [d]Error is the standard deviation of Φ_{coll} measured from four batches of QDs for each s-BQ to account for batch to batch variability in surface ligand density/packing order. [e]Error propagated from errors in k_0 and k_q for a single sample for each monolayer composition.

DOI: 10.1021/jacs.5b13077
J. Am. Chem. Soc. 2016, 138, 2319–2326

electron transfer. We define it using eq 2, where the k_0 is the diffusion limited quenching constant defined by eq 3, and

$$\Phi_{coll} = \frac{k_q}{k_0} \quad (2)$$

$$k_0 = \frac{4\pi N_A}{1000} R_C D_s \quad (3)$$

k_q is extracted from the fits of the data in Figure 3A–D to eq 1. In eq 3, R_c is the radius of collision between a thiolate-treated PbS QD and a freely diffusing Me_4BQ or Me_2BQ molecule, which we define as the sum of their hydrodynamic radii, and D_s is the diffusion constant of Me_4BQ or Me_2BQ in benzene. We determine both quantities with diffusion-ordered spectroscopy (DOSY) NMR (see the Supporting Information, Figure S13). Table 2 lists the values of k_0 and Φ_{coll} for mixtures of Me_4BQ or Me_2BQ with PbS QDs of each PFDT/OA and DT/OA ligand composition.

The reported values of collisional quenching efficiency indicate that only a small fraction (<1%) of collisions between the QDs and solution phase s-BQ molecules results in a quenching event, because the ligand shell acts as an effective barrier to permeation of s-BQ to the QD surface. For the pure OA monolayer (0 PFDT/DT in Table 2), the efficiency of the collisional quenching process, Φ_{coll}, for the QD-Me_2BQ system is a factor of 6 higher than that for the QD-Me_4BQ system. This behavior agrees with previous results on these systems, and indicates that the permeability of the ligand shell is sensitive to even the small change in the molecular volume on going from Me_2BQ (210 Å^3) to Me_4BQ (255 Å^3), as calculated on DFT-optimized structures.[11]

To more clearly illustrate the relationship between the composition and the permeability of the mixed monolayer ligand shells, we use the quantity Φ/Φ_0, where Φ is the value of Φ_{coll} for PbS QDs coated with DT/OA or PFDT/OA mixed monolayers and Φ_0 is value of Φ_{coll} for the PbS QDs coated exclusively with OA. The smaller Φ/Φ_0, the more effectively the ligand shell protects the QD. Figure 4 is a plot of Φ/Φ_0 vs the surface density of thiolates within each type of thiolate/OA mixed monolayer. For a given quencher and a given surface density of thiolate, introducing PFDT into the monolayer is always more effective than introducing DT into the monolayer

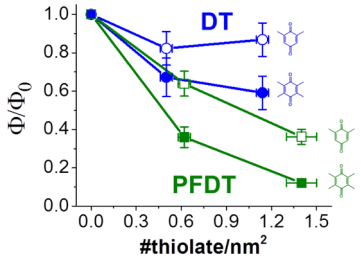

Figure 4. Plots of the ratio of Φ_{coll} at each surface coverage of thiol versus the Φ_{coll} of oleate capped PbS QDs (Φ/Φ_0) for the Me_4BQ (closed symbol) and Me_2BQ (open symbol) quenchers for PbS QDs as a function of PFDT (green) and DT (blue) thiolate surface coverage. Lines are included as a guide to the eye. Vertical error bars are calculated by propagating the error in Φ and Φ_0 from Table 2, in which the error in Φ is calculated from the errors of k_q and k_0, and the error of Φ_0 is reported as the standard deviation of the collisional quenching efficiency of oleate capped PbS QDs measured for four batches of QDs for each quencher.

at reducing the permeability of the ligand shell. For example, reducing Φ_{coll} for the Me_4BQ quencher to ~60% of its value for the all-OA ligand shell requires a surface coverage of ~1.1 DT/nm^2, but a surface coverage of only ~0.43 PFDT/nm^2 (if we linearly interpolate between the data points in Figure 4). Furthermore, regardless of surface density, incorporating DT into the monolayer reduces Φ_{coll} for the Me_2BQ quencher to a minimum of 85% of its value for the all-OA ligand shell, while a surface coverage of 1.4 PFDT/nm^2 reduces Φ_{coll} for Me_2BQ to ~36% of its original value. We constructed an analogous plot to that in Figure 4 where Φ/Φ_0 is calculated from changes in the PbS excited state lifetime rather than changes in the PL intensity of the sample for the PFDT/OA mixed monolayers. The results using the two methods are very similar (see the Figures S14 and S15 in the Supporting Information).

Factors That Determine the Relative Permeabilities of DT/OA and PFDT/OA Mixed Monolayers. The ability of monolayers that contain PFDT to block the permeation of s-BQ molecules more effectively than do monolayers containing DT is probably due to a combination of (i) van der Waals interactions (the greater oleophobicity of PFDT than DT), and (ii) steric bulk (the greater molecular volume and rigidity of PFDT than DT).

To explore the relative impacts of van der Waals interactions and steric bulk of the fluorinated ligands on the permeability of the QD's organic adlayer, we estimated the partition coefficient P of the s-BQs between benzene (the solvent for the PL experiments) and either hexanes (an unbound version of the DT ligand shell) or perfluorohexanes (an unbound version of the PFDT ligand shell), Table 3. We use P as an indicator of the probability that the s-BQ molecules enter the QD ligand shell from the benzene solvent, based only on van der Waals interactions. To measure P, we added an excess of each s-BQ to benzene, hexanes, or perfluorohexanes, and determined the saturated concentration by ^{1}H NMR relative to a biphenyl standard after filtering. We then approximated P as the ratio of the solubility of the s-BQ in either hexanes or fluorohexanes to the solubility of the s-BQ in benzene (in which [s-BQ] is the measured concentration at saturation), eq 4, and used it to estimate the free energy of transferring the s-BQ molecule into the ligand shell (ΔG_{trans}, eq 5).[70−72] Table 3 lists the results of these experiments.

$$P = \frac{[sBQ]_{hx\ or\ fhx}}{[sBQ]_{benzene}} \quad (4)$$

$$\Delta G_{trans} = -RT \ln P \quad (5)$$

Both Me_2BQ and Me_4BQ are poorly solubilized by perfluorohexanes relative to hexanes; so in both cases, the ΔG_{trans} (benzene → perfluorohexanes) is 10 kJ/mol larger than ΔG_{trans} (benzene → hexanes). On the basis of the relative solubilities of Me_2BQ and Me_4BQ in the three solvents, the equilibrium concentration of s-BQ that exists inside the portions of the ligand shell comprising PFDT is a factor of 54−59 lower than the concentration in regions of the ligand shell comprising DT. Collisional quenching efficiency is, to first approximation, directly proportional to the concentration of quenchers within some contact radius of the QD surface.[73] Our solubility results therefore imply that, if the protective qualities of the PFDT shell were only due to its oleophobicity, it should reduce the collisional quenching efficiency (from that of the same coverage of DT) by the same degree (within ~10%) for both Me_2BQ and Me_4BQ. Van der Waals interactions alone therefore do not

DOI: 10.1021/jacs.5b13077
J. Am. Chem. Soc. 2016, 138, 2319−2326

Table 3. Solubility of s-BQs in Benzene, Hexanes, and Perfluorohexanes

	solubility (mg/mL)			ΔG_{trans} (kJ/mol)	
	benzene	hexanes	perfluorohexanes	benzene → hexanes	benzene → perfluorohexanes
Me_2BQ	475	27.6	0.52	+7.0	+16.9
Me_4BQ	275	25.1	0.43	+6.0	+16.0

account for the large differences in the plots of Φ/Φ_0 vs PFDT coverage for Me_4BQ and Me_2BQ. For example, this solubility data cannot explain why, if we again interpolate between data points in Figure 4, the difference in collisional quenching efficiencies of the PFDT and DT monolayers (for a surface coverage of ∼1.1 thiolate/nm^2) is a factor of 3 for the QD/Me_4BQ system, but only a factor of 2 for the QD/Me_2BQ system.

We therefore hypothesize that addition of PFDT to the ligand shell decreases its permeability to s-BQ due to both its oleophobicity and through size exclusion. It is not geometrically possible for the PFDT monolayer to be as densely packed (throughout its thickness) on the high-curvature surface of the QD as it is on planar crystalline metal, but it can still adopt a rigid, helical conformation, which occupies a larger volume than does its aliphatic counterpart.[23,24,26−29,74−76] In addition, the rigid fluoroalkane backbone is less likely to promote either static or dynamic disorder in the adlayer than is the more flexible aliphatic backbone, which is prone to the formation of *gauche* defects, especially on a highly curved surface.[48,49]

Because only a small amount of oleate need be displaced by PFDT in order to profoundly change the collisional quenching efficiency of the QD/Me_2BQ and QD/Me_4BQ systems, we suspect that there are patches of fluorinated ligand distributed throughout the QD surface within these ligand shells.[52,53,77] If instead the PFDT and OA portions of the mixed monolayer were completely phase-segregated, then we hypothesize that displacing the oleate ligands covering 21% of the surface with PFDT should result in approximately a 21% decrease in Φ_{coll}. Instead, we observe that 21% oleate displacement results in a 68% decrease in the Φ_{coll} of Me_4BQ. We have not measured the distribution of PFDT and OA in these mixed monolayers directly, but this nonlinear response of Φ_{coll} to PFDT coverage suggests that the structure of the partially fluorinated ligand layer is a kinetically trapped mixture, that is, dictated by random, irreversible binding of the PFDT ligand, rather than a phase segregated, thermodynamically controlled configuration.[78−81]

CONCLUSIONS

In summary, we used a combination of NMR, photoluminescence, and transient absorption spectroscopies to demonstrate that introducing the fluorinated thiol PFDT into the oleate ligand shell on the surfaces of PbS quantum dots is more effective at reducing the permeability of this organic adlayer to solution phase quenchers than is doping the monolayer with the corresponding aliphatic thiol. As probed by the yield of interfacial electron transfer between the QD and a substituted benzoquinone photo-oxidant (Me_4BQ or Me_2BQ), introducing PFDT into the oleate ligand layer at a surface density of 0.62 PFDT/nm^2 (approximately 21% surface coverage) reduces the probability that Me_4BQ will permeate the ligand shell (upon collision with its outer surface) by ∼65%, and a surface density of 1.4 PFDT/nm^2 (approximately 42% surface coverage) reduces this probability by ∼90%. We determined that the protective properties of the PFDT-doped monolayer are due to both the oleophobicity and the steric bulk and rigidity of the PFDT ligand, and that the PFDT ligands probably exist in small clusters spread homogeneously over the QD surface.

We note that in this analysis, we have not explicitly addressed a theoretical result that indicates that the distance dependence of charge transfer reactions can take different functional forms depending on the driving force for the reaction.[82] This result would complicate our interpretation, as the driving forces for electron transfer from the QD to Me_4BQ and Me_2BQ differ by 0.2 eV; so in principle, the inclusion of PFDT into the ligand shell could prevent Me_4BQ and Me_2BQ from reaching the surface of the nanocrystal to the same extent, but result in slightly different mean donor−acceptor distances for the two molecules. We do not believe this consideration is relevant here, however. We have shown in previous work on PbS QD-s-BQ systems that the collisional quenching efficiency for two s-BQs with very similar driving forces but different molecular volumes are different; the bulkier s-BQ had a lower collisional quenching efficiency than the less-bulky s-BQ.[11] We are therefore confident in treating the collisional quenching efficiency as a metric for ligand shell permeability in these particular collisionally gated reactions.

This work expands the toolset for controlling the redox activity of nanocrystals via fluorination of the ligand shell, and is therefore also relevant for the development of semiconductor nanocrystals with enhanced resistance to redox- and photo-redox-mediated corrosion, a useful property for applications in solid-state lighting and photocatalysis. The small portion of the monolayer that requires fluorination in order to impart stability implies that we can synthesize highly chemically inert water-soluble PbS QDs as biocompatible emissive tags[41,42] or multimodal ^{19}F MRI/optical tags,[44] with emission tuned to the so-called "NIR water window" for high fidelity biological imaging.

Finally, we have again[11,55,63] demonstrated the utility and sensitivity of photoinduced electron transfer experiments in probing the intermolecular structure of the QD ligand shell, which is complicated to interrogate using traditional analytical methods. The yield of collisional electron transfer, as measured simply by photoluminescence, is sensitive not only to the chemical composition of the organic adlayer, but also to its morphology, which is rarely examined in systems of nanocrystals coated with mixed monolayers. We hope these studies will inform the rational design of robust QD emitters and sensing platforms.

ASSOCIATED CONTENT

Supporting Information

The Supporting Information is available free of charge on the ACS Publications website at DOI: 10.1021/jacs.5b13077.

Details of synthesis and sample preparation; transmission electron microscopy; ^{1}H NMR and ^{19}F NMR ligand shell quantification; supporting photoluminescence and transient absorption experiments; diffusion ordered spectroscopy (DOSY); alternate construction of Φ/Φ_0 plot from transient absorption data (PDF)

DOI: 10.1021/jacs.5b13077
J. Am. Chem. Soc. 2016, 138, 2319−2326

AUTHOR INFORMATION

Corresponding Author

*e-weiss@northwestern.edu

Notes

The authors declare no competing financial interest.

ACKNOWLEDGMENTS

This work was supported by the National Science Foundation (Award No. 1400596) to E.A.W. D.J.W. was funded by the Department of Energy Office of Science Graduate fellowship program (DOE SCGF), which was administered by ORISE-ORAU under contract number DE-AC05-06OR23100 for part of this work. NMR measurements were performed at Northwestern University's Integrated Molecular Structure Education and Research Center (IMSERC). Electron microscopy was performed in the NU*ANCE* Center at Northwestern University. NUANCE is supported by the International Institute for Nanotechnology, MRSEC (NSF DMR-1121262), the Keck Foundation, the State of Illinois, and Northwestern University.

REFERENCES

(1) Wang, H. F.; He, Y.; Ji, T. R.; Yan, X. P. *Anal. Chem.* **2009**, *81*, 1615.
(2) Medintz, I. L.; Uyeda, H. T.; Goldman, E. R.; Mattoussi, H. *Nat. Mater.* **2005**, *4*, 435.
(3) Knowles, K. E.; Peterson, M. D.; McPhail, M. R.; Weiss, E. A. *J. Phys. Chem. C* **2013**, *117*, 10229.
(4) Watson, D. F. *J. Phys. Chem. Lett.* **2010**, *1*, 2299.
(5) Nevins, J. S.; Coughlin, K. M.; Watson, D. F. *ACS Appl. Mater. Interfaces* **2011**, *3*, 4242.
(6) Peveler, W. J.; Roldan, A.; Hollingsworth, N.; Porter, M. J.; Parkin, I. P. *ACS Nano* **2016**, *10*, 1139.
(7) Freeman, R.; Finder, T.; Bahshi, L.; Willner, I. *Nano Lett.* **2009**, *9*, 2073.
(8) Suzuki, M.; Husimi, Y.; Komatsu, H.; Suzuki, K.; Douglas, K. T. *J. Am. Chem. Soc.* **2008**, *130*, 5720.
(9) Liu, J. W.; Lee, J. H.; Lu, Y. *Anal. Chem.* **2007**, *79*, 4120.
(10) Klein, E.; Kerth, P.; Lebeau, L. *Biomaterials* **2008**, *29*, 204.
(11) Knowles, K. E.; Tagliazucchi, M.; Malicki, M.; Swenson, N. K.; Weiss, E. A. *J. Phys. Chem. C* **2013**, *117*, 15849.
(12) Love, J. C.; Estroff, L. A.; Kriebel, J. K.; Nuzzo, R. G.; Whitesides, G. M. *Chem. Rev.* **2005**, *105*, 1103.
(13) Bain, C. D.; Whitesides, G. M. *J. Am. Chem. Soc.* **1989**, *111*, 7164.
(14) Laibinis, P. E.; Nuzzo, R. G.; Whitesides, G. M. *J. Phys. Chem.* **1992**, *96*, 5097.
(15) Atre, S. V.; Liedberg, B.; Allara, D. L. *Langmuir* **1995**, *11*, 3882.
(16) Doneux, T.; Steichen, M.; Bouchta, T.; Buess-Herman, C. *J. Electroanal. Chem.* **2007**, *599*, 241.
(17) Chapman, R. G.; Ostuni, E.; Yan, L.; Whitesides, G. M. *Langmuir* **2000**, *16*, 6927.
(18) Deng, L.; Mrksich, M.; Whitesides, G. M. *J. Am. Chem. Soc.* **1996**, *118*, 5136.
(19) Porter, M. D.; Bright, T. B.; Allara, D. L.; Chidsey, C. E. D. *J. Am. Chem. Soc.* **1987**, *109*, 3559.
(20) Evans, S. D.; Urankar, E.; Ulman, A.; Ferris, N. *J. Am. Chem. Soc.* **1991**, *113*, 4121.
(21) Tamchang, S. W.; Biebuyck, H. A.; Whitesides, G. M.; Jeon, N.; Nuzzo, R. G. *Langmuir* **1995**, *11*, 4371.
(22) Ulman, A. *Chem. Rev.* **1996**, *96*, 1533.
(23) Zenasni, O.; Jamison, A. C.; Lee, T. R. *Soft Matter* **2013**, *9*, 6356.
(24) Chidsey, C. E. D.; Loiacono, D. N. *Langmuir* **1990**, *6*, 682.
(25) Barriet, D.; Lee, T. R. *Curr. Opin. Colloid Interface Sci.* **2003**, *8*, 236.
(26) Lu, H.; Zeysing, D.; Kind, M.; Terfort, A.; Zharnikov, M. *J. Phys. Chem. C* **2013**, *117*, 18967.
(27) Weinstein, R. D.; Moriarty, J.; Cushnie, E.; Colorado, R.; Lee, T. R.; Patel, M.; Alesi, W. R.; Jennings, G. K. *J. Phys. Chem. B* **2003**, *107*, 11626.
(28) Naud, C.; Calas, P.; Commeyras, A. *Langmuir* **2001**, *17*, 4851.
(29) Tsao, M. W.; Hoffmann, C. L.; Rabolt, J. F.; Johnson, H. E.; Castner, D. G.; Erdelen, C.; Ringsdorf, H. *Langmuir* **1997**, *13*, 4317.
(30) Chau, L. K.; Porter, M. D. *Chem. Phys. Lett.* **1990**, *167*, 198.
(31) Alves, C. A.; Porter, M. D. *Langmuir* **1993**, *9*, 3507.
(32) Shaporenko, A.; Cyganik, P.; Buck, M.; Ulman, A.; Zharnikov, A. *Langmuir* **2005**, *21*, 8204.
(33) Krafft, M. P.; Riess, J. G. *Biochimie* **1998**, *80*, 489.
(34) Babudri, F.; Farinola, G. M.; Naso, F.; Ragni, R. *Chem. Commun.* **2007**, 1003.
(35) Wong, T. S.; Kang, S. H.; Tang, S. K. Y.; Smythe, E. J.; Hatton, B. D.; Grinthal, A.; Aizenberg, J. *Nature* **2011**, *477*, 443.
(36) Epstein, A. K.; Wong, T. S.; Belisle, R. A.; Boggs, E. M.; Aizenberg, J. *Proc. Natl. Acad. Sci. U. S. A.* **2012**, *109*, 13182.
(37) Yao, X.; Dunn, S. S.; Kim, P.; Duffy, M.; Alvarenga, J.; Aizenberg, J. *Angew. Chem., Int. Ed.* **2014**, *53*, 4418.
(38) Song, W.; Rossky, P. J.; Maroncelli, M. *J. Chem. Phys.* **2003**, *119*, 9145.
(39) Liao, K. C.; Bowers, C. M.; Yoon, H. J.; Whitesides, G. M. *J. Am. Chem. Soc.* **2015**, *137*, 3852.
(40) Dalvi, V. H.; Rossky, P. J. *Proc. Natl. Acad. Sci. U. S. A.* **2010**, *107*, 13603.
(41) Euliss, L. E.; Nosho, B.; Abueg, N. L.; Granger, M. G.; Brewer, P. D.; Behroozi, M. US Patent, US 20140079912 A1, 2012.
(42) Breen, C.; Steckel, J. S. US Patent, US 20140027711 A1, 2011.
(43) Qian, C. X.; Sun, W.; Wang, L. W.; Chen, C. L.; Liao, K.; Wang, W. D.; Jia, J.; Hatton, B. D.; Casillas, G.; Kurylowicz, M.; Yip, C. M.; Mastronardi, M. L.; Ozin, G. A. *J. Am. Chem. Soc.* **2014**, *136*, 15849.
(44) Tirotta, I.; Dichiarante, V.; Pigliacelli, C.; Cavallo, G.; Terraneo, G.; Bombelli, F. B.; Metrangolo, P.; Resnati, G. *Chem. Rev.* **2015**, *115*, 1106.
(45) Lim, Y. T.; Noh, Y. W.; Cho, J. H.; Han, J. H.; Choi, B. S.; Kwon, J.; Hong, K. S.; Gokarna, A.; Cho, Y. H.; Chung, B. H. *J. Am. Chem. Soc.* **2009**, *131*, 17145.
(46) Gorelikov, I.; Martin, A. L.; Seo, M.; Matsuura, N. *Langmuir* **2011**, *27*, 15024.
(47) Colorado, R.; Lee, T. R. *Langmuir* **2003**, *19*, 3288.
(48) Frederick, M. T.; Achtyl, J. L.; Knowles, K. E.; Weiss, E. A.; Geiger, F. M. *J. Am. Chem. Soc.* **2011**, *133*, 7476.
(49) Weeraman, C.; Yatawara, A. K.; Bordenyuk, A. N.; Benderskii, A. V. *J. Am. Chem. Soc.* **2006**, *128*, 14244.
(50) Pengo, P.; Pasquato, L. *J. Fluorine Chem.* **2015**, *177*, 2.
(51) Boccalon, M.; Bidoggia, S.; Romano, F.; Gualandi, L.; Franchi, P.; Lucarini, M.; Pengo, P.; Pasquato, L. *J. Mater. Chem. B* **2015**, *3*, 432.
(52) Posocco, P.; Gentilini, C.; Bidoggia, S.; Pace, A.; Franchi, P.; Lucarini, M.; Fermeglia, M.; Pricl, S.; Pasquato, L. *ACS Nano* **2012**, *6*, 7243.
(53) Gentilini, C.; Franchi, P.; Mileo, E.; Polizzi, S.; Lucarini, M.; Pasquato, L. *Angew. Chem., Int. Ed.* **2009**, *48*, 3060.
(54) Gentilini, C.; Evangelista, F.; Rudolf, P.; Franchi, P.; Lucarini, M.; Pasquato, L. *J. Am. Chem. Soc.* **2008**, *130*, 15678.
(55) Knowles, K. E.; Malicki, M.; Weiss, E. A. *J. Am. Chem. Soc.* **2012**, *134*, 12470.
(56) Hines, M. A.; Scholes, G. D. *Adv. Mater.* **2003**, *15*, 1844.
(57) Moreels, I.; Lambert, K.; Smeets, D.; De Muynck, D.; Nollet, T.; Martins, J. C.; Vanhaecke, F.; Vantomme, A.; Delerue, C.; Allan, G.; Hens, Z. *ACS Nano* **2009**, *3*, 3023.
(58) Marbella, L. E.; Millstone, J. E. *Chem. Mater.* **2015**, *27*, 2721.
(59) Hens, Z.; Martins, J. C. *Chem. Mater.* **2013**, *25*, 1211.
(60) Moreels, I.; Fritzinger, B.; Martins, J. C.; Hens, Z. *J. Am. Chem. Soc.* **2008**, *130*, 15081.
(61) Anderson, N. C.; Hendricks, M. P.; Choi, J. J.; Owen, J. S. *J. Am. Chem. Soc.* **2013**, *135*, 18536.
(62) Cass, L. C.; Malicki, M.; Weiss, E. A. *Anal. Chem.* **2013**, *85*, 6974.
(63) Aruda, K. O.; Bohlmann Kunz, M.; Tagliazucchi, M.; Weiss, E. A. *J. Phys. Chem. Lett.* **2015**, *6*, 2841.

DOI: 10.1021/jacs.5b13077
J. Am. Chem. Soc. 2016, 138, 2319−2326

(64) Wang, G. L.; Jiao, H. J.; Liu, K. L.; Wu, X. M.; Dong, Y. M.; Li, Z. J.; Zhang, C. *Electrochem. Commun.* **2014**, *41*, 47.
(65) Long, D.; Wu, G. Z.; Wang, W. F.; Yao, S. *Res. Chem. Intermed.* **2007**, *33*, 655.
(66) Lou, Y. B.; Chen, X. B.; Samia, A. C.; Burda, C. *J. Phys. Chem. B* **2003**, *107*, 12431.
(67) Burda, C.; Green, T. C.; Link, S.; El-Sayed, M. A. *J. Phys. Chem. B* **1999**, *103*, 1783.
(68) Morris-Cohen, A. J.; Peterson, M. D.; Frederick, M. T.; Kamm, J. M.; Weiss, E. A. *J. Phys. Chem. Lett.* **2012**, *3*, 2840.
(69) Malicki, M.; Knowles, K. E.; Weiss, E. A. *Chem. Commun.* **2013**, *49*, 4400.
(70) Dearden, J. C.; Bresnen, G. M. *Quant. Struct.-Act. Relat.* **1988**, *7*, 133.
(71) Yalkowsky, S. H.; Valvani, S. C.; Roseman, T. J. *J. Pharm. Sci.* **1983**, *72*, 866.
(72) Leo, A.; Hansch, C.; Elkins, D. *Chem. Rev.* **1971**, *71*, 525.
(73) Lakowicz, J. R. In *Principles of Fluorescence Spectroscopy*; Lakowicz, J. R., Ed.; Springer: New York, 2006; p 331.
(74) Bunn, C. W.; Howells, E. R. *Nature* **1954**, *174*, 549.
(75) Krafft, M. P.; Goldmann, M. *Curr. Opin. Colloid Interface Sci.* **2003**, *8*, 243.
(76) Barton, S. W.; Goudot, A.; Bouloussa, O.; Rondelez, F.; Lin, B. H.; Novak, F.; Acero, A.; Rice, S. A. *J. Chem. Phys.* **1992**, *96*, 1343.
(77) Stewart, A.; Zheng, S.; McCourt, M. R.; Bell, S. E. J. *ACS Nano* **2012**, *6*, 3718.
(78) Smith, R. K.; Reed, S. M.; Lewis, P. A.; Monnell, J. D.; Clegg, R. S.; Kelly, K. F.; Bumm, L. A.; Hutchison, J. E.; Weiss, P. S. *J. Phys. Chem. B* **2001**, *105*, 1119.
(79) Stranick, S. J.; Parikh, A. N.; Tao, Y. T.; Allara, D. L.; Weiss, P. S. *J. Phys. Chem.* **1994**, *98*, 7636.
(80) Folkers, J. P.; Laibinis, P. E.; Whitesides, G. M.; Deutch, J. *J. Phys. Chem.* **1994**, *98*, 563.
(81) Stranick, S. J.; Atre, S. V.; Parikh, A. N.; Wood, M. C.; Allara, D. L.; Winograd, N.; Weiss, P. S. *Nanotechnology* **1996**, *7*, 438.
(82) Tachiya, M.; Murata, S. *J. Phys. Chem.* **1992**, *96*, 8441.

DOI: 10.1021/jacs.5b13077
J. Am. Chem. Soc. 2016, 138, 2319−2326